



**HAL**  
open science

# Polyelectrolyte complexes of hyaluronic acid and diethylaminoethyl dextran: Formation, stability and hydrophobicity

Huu Van Le, Virginie Dulong, Luc Picton, Lecerf Didier

► **To cite this version:**

Huu Van Le, Virginie Dulong, Luc Picton, Lecerf Didier. Polyelectrolyte complexes of hyaluronic acid and diethylaminoethyl dextran: Formation, stability and hydrophobicity. *Colloids and Surfaces A: Physicochemical and Engineering Aspects*, 2021, 629, pp.127485. 10.1016/j.colsurfa.2021.127485 . hal-03343724

**HAL Id: hal-03343724**

**<https://hal.science/hal-03343724>**

Submitted on 16 Oct 2023

**HAL** is a multi-disciplinary open access archive for the deposit and dissemination of scientific research documents, whether they are published or not. The documents may come from teaching and research institutions in France or abroad, or from public or private research centers.

L'archive ouverte pluridisciplinaire **HAL**, est destinée au dépôt et à la diffusion de documents scientifiques de niveau recherche, publiés ou non, émanant des établissements d'enseignement et de recherche français ou étrangers, des laboratoires publics ou privés.



Distributed under a Creative Commons Attribution - NonCommercial 4.0 International License

# **Polyelectrolyte complexes of hyaluronic acid and diethylaminoethyl dextran: formation, stability and hydrophobicity**

Huu Van LE, Virginie DULONG, Luc PICTON, Didier LE CERF \*

*Normandie Univ, UNIROUEN, INSA Rouen, CNRS, PBS UMR 6270, 76000 Rouen, France*

\*Corresponding author: E-mail address: [didier.lecerf@univ-rouen.fr](mailto:didier.lecerf@univ-rouen.fr)

Tel: 00 33 02 35 14 65 43; Fax: 00 33 02 35 14 67 04

## ABSTRACT

Polyelectrolyte complexes (PECs) of hyaluronic acid (HA) and diethylaminoethyl dextran (DEAE-D), promising for biomedical applications, have been investigated with respect to physicochemical properties, mainly in terms of particle size and relative hydrophobicity as well as storage stability. Influences of charge ratio, polymer concentration, molar masses of HA, ionic strength and mixing methods have been particularly investigated. The complexation between HA and DEAE-D generally resulted in colloidal particles having mean hydrodynamic diameter of 150-350 nm, with larger particle size observed at negative to positive charge ratio ( $n^-/n^+$ ) further from the unity. Higher polymer concentration or higher molar mass of HA also led to higher particle size of the PECs, whereas the increasing ionic strength led to a non-monotonic evolution in particle size. The effects of mixing mode and mixing order on particle size were interdependent and depended also on  $n^-/n^+$ . PECs at  $n^-/n^+ \leq 0.4$  showed lack of stability, which seemed not to be sensitive to storage temperature but significantly improved at higher salt concentration or lower polymer concentration. The relative hydrophobicity of such PECs was also confirmed by the fluorescence spectra of pyrene incorporated in PEC particles. Such results gave a better insight to polysaccharides-based PECs, especially as a potential system to encapsulate hydrophobic active molecules for drug delivery purposes.

Keywords: polyelectrolyte complexes; hyaluronic acid; diethylaminoethyl dextran, polysaccharide; pyrene fluorescence

## 1. Introduction

Polyelectrolyte complexes (PECs), sometimes referred as polyion complexes, are formed by self-assembly of oppositely charged polymers, i.e. polyanions and polycations. The formation of PECs in aqueous media is consensually regarded as an entropy-driven phenomenon, as the association between polyanions and polycations occurs by means of electrostatic interactions (Coulomb forces) with the main driving force being the increase in entropy due to the release of water molecules and counter-ions [1, 2]. Hydrogen bonding, hydrophobic interactions and van der Waals forces can also be involved in PECs formation [3, 4].

Different kinds of PECs can be elaborated with different possible morphologies, including water-soluble PECs, colloidal PECs, PEC coacervates and solid PECs or precipitates. These morphologies as well as their phase behaviours vary widely depending on the balance of the polyelectrolytes, salt ions and water within the complex, which is directly related to several factors: total polymer concentration ( $C_P$ ) and polymer molar mass, salt concentration, electrostatic interaction strength, charge density and charge ratio, i.e. molar ratio between negative and positive charges ( $n^-/n^+$ ), which is usually related to the pH of reaction media [4-8]. Complexation of low molar mass polyelectrolytes having weak ionic groups and a large difference in chain lengths at a non-stoichiometric mixing ratio would favourably generate soluble PECs which could be compared to chains of block copolymer with neutralized segments as hydrophobic blocks and unpaired segments as hydrophilic blocks, or colloidal stable PECs usually described as particles with neutral and hydrophobic cores surrounded by hydrophilic and polar shells [4, 6, 9]. On the contrary, high and similar molar masses, strong charge-charge interactions and stoichiometric mixing of the complexing polyelectrolytes usually favour aggregation, phase separation and precipitation of PECs [4, 9]. Also, PEC morphology is

possibly influenced by preparation parameters such as mode of mixing (e.g. rapid one-shot or slow dropwise addition) and order of addition [6, 10]. A comprehensive and in-depth understanding of these factors as well as their intercorrelation may therefore allow the tunability of PECs in terms of physicochemical properties for a wide range of applications, e.g. biomedicine, pharmaceuticals, nutraceuticals, cosmetics, food and paper industries [9, 11, 12].

For healthcare applications, PECs from biopolymers usually attract more interest compared with those of synthetic polyelectrolytes, since the formers are generally more biocompatible and biodegradable [13]. Accordingly, biomaterials-based PECs from polysaccharides, proteins or polypeptides have been extensively reported in the literature [14, 15]. Among several biopolymers employed so far for such applications, hyaluronic acid (HA) has attracted a great deal of attention due to its excellent biocompatibility, stemming from the fact that HA is naturally found in the human body [16]. HA has also been widely used as ligand in drug delivery systems to target tumours *via* the relevant CD44 receptors on tumour cells [17]. Owing to the carboxylic groups of the D-glucuronic acid in its structure, HA would display negative charge in aqueous media at certain pH range and thus form PECs upon mixing with positively charged polymers. Typically, PECs from HA and polycations, most commonly chitosan (CS), have become the topic of great interest for clinical and biomedical applications. For instance, solid HA/CS PECs were elaborated as nasal insert encapsulating vancomycin and insulin [18]. Coacervates of HA and lactose-modified CS were also studied for radical-scavenging activities [19]. HA/CS nanoparticles for curcuminoid delivery in glioma cells were also reported [20].

While such studies of PECs from HA and CS are abundant, there has been less research focusing on the complexation between HA and other positively charged biopolymers. Specifically, to the best of our knowledge, no studies so far have focused on PECs prepared from HA and

diethylaminoethyl dextran (DEAE-D). DEAE-D is a polycationic derivative of dextran, a natural and more flexible polysaccharide than CS. The most studied application of DEAE-D is its capacity to form complexes with negatively charged biomacromolecules like nucleic acids and proteins for nucleic acid transfection or to provide sustained-release protein delivery [21, 22]. DEAE-D can also be used as coating agent for nano/microparticles in drug delivery systems due to its stabilizing effects [23, 24]. Furthermore, DEAE-D itself could exert therapeutic effects, namely inhibition of tumour growth [25, 26]. Like CS, DEAE-D is also a low-cost polysaccharide with satisfactory biocompatibility and biodegradability. The advantage of DEAE-D over CS lies in its good solubility in aqueous solutions at any pH which renders DEAE-D more favourable in certain cases, for example when neutral or high pH is needed [23].

With their opposite charges in aqueous media, HA and DEAE-D must form PECs through ion-pairing (**Figure 1**). The aim of this study was to investigate the HA/DEAE-D complexation by evaluating the impact of different parameters involved in the complexation process. The resulting systems were evaluated in terms of morphology through their visual aspect and physicochemical characteristics of PEC nanoparticles including particle size, particle concentration, particle net surface charge and the stability of particle size, as well as their potential hydrophobicity. This would allow a better insight into PECs structures and behaviours, which is associated with optimizing the relevant parameters for elaboration of nanocarriers encapsulating therapeutic agents.

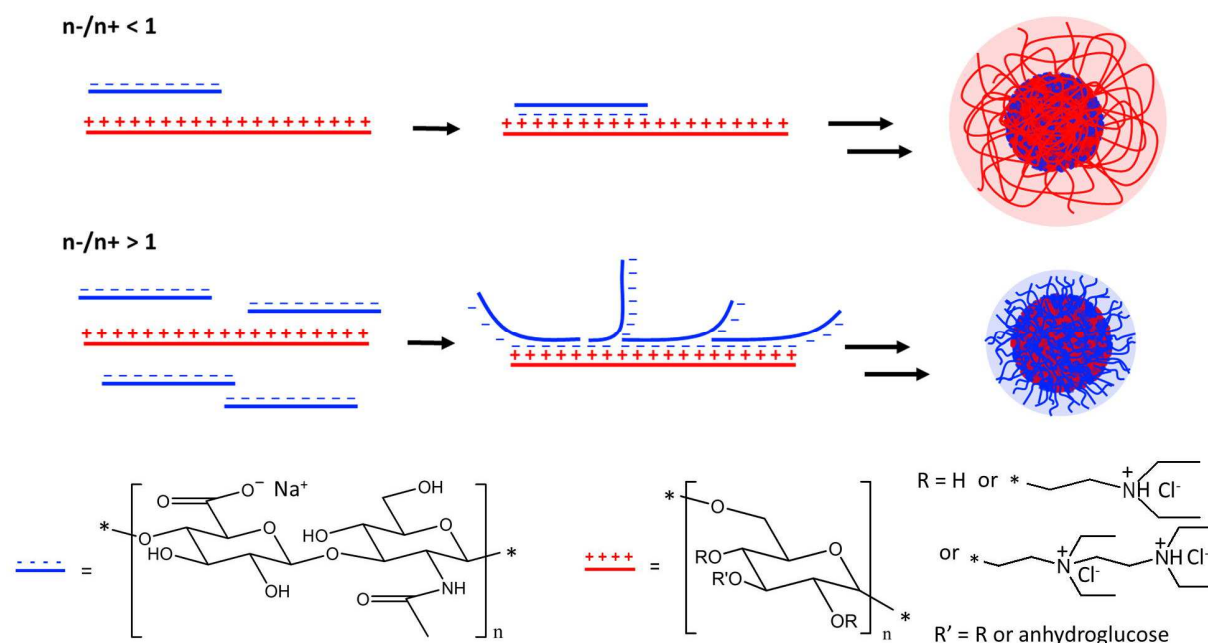


**Figure 1.** Schematic illustration of the complexation between HA as polyanion (blue) and DEAE-D of higher molar mass as polycation (red), in case of polycation in excess ( $n-/n+ < 1$ ) or polyanion in excess ( $n-/n+ > 1$ ). The double strain segments in the primary complexes formed by ion-pairing could be relatively hydrophobic. The aggregation of primary complexes through intercomplex interactions (including electrostatic and hydrophobic interactions, van der Waals forces and hydrogen bonding) could finally lead to particles with relatively hydrophobic cores and highly hydrophilic shells.

## 2. Materials and methods

### 2.1. Materials

Medium- and high-molar-mass sodium hyaluronates ( $\text{HA}_M$  and  $\text{HA}_H$  respectively) with purity over 95% were kindly provided by Givaudan (France). DEAE-D hydrochloride and polyethyleneimine (PEI) hydrochloride were purchased from Sigma-Aldrich (USA). The macromolecular characteristics of HAs and DEAE-D were obtained by size exclusion chromatography coupled with multi-angle light scattering, differential refractive index and viscosity detectors (see Appendix). The ionization rate ( $\alpha$ ) of HA units (number of deprotonated

carboxylic groups per D-glucuronic-N-acetylglucosamine unit) in function of pH was calculated from the modified Henderson-Hasselbalch (**Equation 1**):

$$\text{pH} = \text{pKa} + \log[\alpha/(1 - \alpha)] \quad \text{(Equation 1)}$$

with pKa of HA equal to 2.9, obtained from HA having comparable molar mass reported in the literature [27]. For DEAE-D, the degree of substitution per anhydroglucose unit of quaternary amino groups (0.26) and of tertiary amino groups (0.29) as well as the ionization rate of anhydroglucose units in function of pH were reported in our previous studies [28]. All data are summarized in **Table 1** and **Figure 2**. Pyrene with purity of 98% was purchased from Acros Organics (USA). Sodium chloride (NaCl), hydrochloric acid (HCl), sodium hydroxide (NaOH) and acetone were purchased from VWR (France). Water used for all experiments was purified with Milli-Q system (Millipore, USA).

**Table 1.** Macromolecular characteristics of polyelectrolytes

Samples	$M_n$ (g.mol <sup>-1</sup> )	$M_w$ (g.mol <sup>-1</sup> )	$\mathcal{D}$	$R_{g_w}$ (nm)
HA <sub>M</sub>	210 000	270 000	1.3	53
HA <sub>H</sub>	670 000	830 000	1.2	115
DEAE-D	270 000	700 000	2.6	29
PEI <sup>(a)</sup>	12 586	-	1.3	-

$M_n$ : number average molar mass;  $M_w$ : weight average molar mass;  $\mathcal{D}$ : dispersity;  $R_{g_w}$ : weight average gyration radius; <sup>(a)</sup> Supplier data

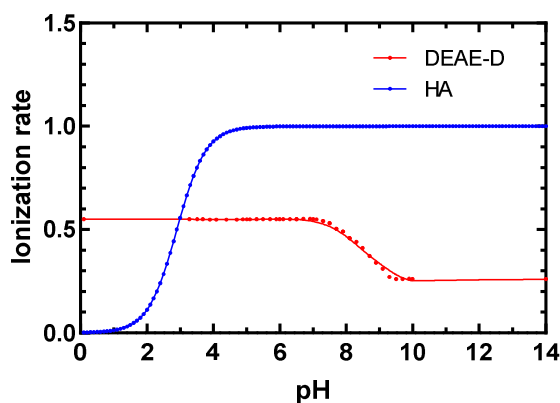


**Figure 2.** Ionization rate of HA units (D-glucuronic-N-acetylglucosamine) and DEAE-D units (anhydroglucose) in function of pH

## 2.2. PECs preparation and storage

Polyelectrolyte solutions were prepared by dissolving the polymers in aqueous solvents of interest under stirring at 200 rpm for one night at room temperature before complexation experiments. Depending on each study, the aqueous solvents used were Milli-Q water, NaCl solutions at various concentration or pyrene  $4 \times 10^{-7} \text{ mol.L}^{-1}$ .  $C_P$  was varied from 0.25 to  $1 \text{ g.L}^{-1}$ . The pH of polymer solutions was measured by using a pH meter equipped with a LE438 electrode (Mettler Toledo, Switzerland). All polyelectrolyte solutions were thereafter filtered through  $0.45 \mu\text{m}$  regenerated cellulose membrane filter units (Sartorius, Germany). The complexations were performed by mixing the polyanion and polycation solutions of the same  $C_P$  and solvent under mild stirring (200 rpm) at room temperature. Unless otherwise stated, the usual mixing method was a rapid one-shot dropping of the polyanion in the polycation using a micropipette. The total stirring time from the beginning of mixing and the total volume of complexations were 30 min and 5 mL, respectively. The volume ratios between the two polymer solutions were varied and calculated from the target  $n^-/n^+$  by using **Equation 2**:

$$n^-/n^+ = (\alpha^- V^- C^- M_0^+) / (\alpha^+ V^+ C^+ M_0^-) \quad \text{(Equation 2)}$$

with  $\alpha$ ,  $V$ ,  $C$  and  $M_0$  being respectively unit ionization rate, solution volume (mL), polymer solution concentration ( $\text{g}\cdot\text{L}^{-1}$ ) and unit average molar mass ( $\text{g}\cdot\text{mol}^{-1}$ ) of the polyanion (-) and the polycation (+).  $M_0$  for (D-glucuronic-N-acetylglucosamine) units of HA and anhydroglucose units of DEAE-D were 378 and 217  $\text{g}\cdot\text{mol}^{-1}$ , respectively.  $\alpha$  values of HA and DEAE-D units at defined pH values were obtained from **Figure 2** and were at their maxima (1 and 0.55 respectively) in Milli-Q water (pH = 5-6). For stability studies, PECs were stored either at 4 °C or at 25 °C following their first characterizations for evaluation of particle size stability after 1, 3, 7 and 30 days. All experiments were carried out at least three times.

### ***2.3. Particle size, particle concentration and zeta potential measurement***

Particle size, particle concentration and zeta potential (i.e. electrophoretic mobility) characterizations were carried out using Zetasizer Ultra instrument (Malvern Panalytical, UK) for visually homogeneous PECs samples without further dilution. Particle size as average hydrodynamic diameter ( $D_h$ ), polydispersity index (PDI) and total particle concentration (TPC) were determined by dynamic light scattering (DLS) technique. For the measurements of  $D_h$  and PDI, at least 1 mL of samples was placed in a two-clear sided plastic cuvette (VWR, France) and back scatter was set as angle of detection. For the measurements of TPC, at least 1 mL of samples was placed in a four-clear sided plastic cuvette (Brand, Germany) as the process required back scatter, side scatter and forward scatter detections. Zeta potential ( $\zeta$ ) was measured by electrophoretic light scattering technique with samples placed in a plastic folded capillary cell (Malvern Panalytical, UK). For each sample, at least three measurements were performed at 25 °C after 120 seconds of temperature stabilization. The measurement data were processed on ZS XPLOERER v1.2.0.91 software.

#### 2.4. Pyrene fluorescence studies

Samples preparation: A stock solution having pyrene concentration ( $C_{Py}$ ) of  $10^{-3}$  mol.L<sup>-1</sup> in acetone was prepared and stored at 4 °C. In order to prepare pyrene  $4 \times 10^{-7}$  mol.L<sup>-1</sup> and  $8 \times 10^{-7}$  mol.L<sup>-1</sup> aqueous solutions, 10  $\mu$ L and 20  $\mu$ L aliquots of the stock solution were introduced to 50 mL volumetric flasks respectively, which were then filled with Milli-Q water after complete acetone evaporation and stirred for 24 h. Samples of HA<sub>M</sub>/DEAE-D PECs containing pyrene (HA<sub>M</sub>/DEAE-D/Py) at  $C_{Py} = 4 \times 10^{-7}$  mol.L<sup>-1</sup> were then prepared for  $C_P = 0.25$  and  $0.5$  g.L<sup>-1</sup> by either: (a) mixing the pyrene  $8 \times 10^{-7}$  mol.L<sup>-1</sup> aqueous solution with the same volume of PEC suspensions with  $C_P = 0.5$  and  $1$  g.L<sup>-1</sup> respectively or (b) complexation upon mixing polyelectrolyte solutions with  $C_P = 0.25$  and  $0.5$  g.L<sup>-1</sup> readily prepared in pyrene  $4 \times 10^{-7}$  mol.L<sup>-1</sup> aqueous solution. All samples were stirred at 200 rpm at room temperature overnight before fluorescence measurements. All samples were prepared in triplicate.

Fluorescence measurements: Fluorescence measurements were carried out at room temperature with a Fluoromax-4 spectrofluorometer (Horiba Jobin Yvon, France). The fluorescence emission spectra ( $\lambda_{em} = 350-450$  nm) were obtained with excitation wavelength  $\lambda_{ex} = 335$  nm. The ratio  $I_I/I_{III}$  was calculated as the intensity ratio between the first and third vibronic bands recorded respectively at 373 nm and 383 nm in the emission spectra [29, 30]. The fluorescence excitation spectra ( $\lambda_{ex} = 300-360$  nm) were also recorded at emission wavelength  $\lambda_{em} = 373$  nm. The ratio  $I_{335}/I_{338}$  was calculated as the intensity ratio between the bands recorded respectively at 335 nm and 338 nm in the excitation spectra [31, 32]. Polyelectrolyte solutions containing pyrene at the same concentrations were also measured as references. All measurements were done at least three times for each sample.

### 3. Results and discussion

#### 3.1. Influences of different factors on PECs formation

In this section, HA/DEAE-D PECs were evaluated in terms of suspension visual aspect, particle size (hydrodynamic diameter,  $D_h$ ) and particle size distribution (polydispersity index, PDI), particle amount (total particle concentration, TPC) and net surface charge (zeta potential,  $\zeta$ ) after 30 minutes of complexation. The PECs were prepared with different varied intrinsic parameters including charge ratio, polymers concentration, polymer molar mass (i.e. HA molar mass), ionic strength and experimental parameters (i.e. mixing mode and mixing order) in order to study their influences on the PECs.

##### 3.1.1. Influence of charge ratio

The impact of  $n^-/n^+$  ratio, from 0.1 to 10, has been studied for  $HA_M/DEAE-D$  PECs with  $C_P = 0.5 \text{ g}\cdot\text{L}^{-1}$  in Milli Q water. Before the complexation, the pHs of HA and DEAE-D  $0.5 \text{ g}\cdot\text{L}^{-1}$  solutions were  $5.7 \pm 0.2$  and  $4.4 \pm 0.2$  respectively, implying their maximal ionization rate (1 and 0.55 respectively) as shown in **Figure 2**. At the beginning of the complexation (polyanion in polycation), a visible turbidity was observed immediately following the mixing of the two polyelectrolytes, indicating an instantaneous formation of PECs. This could be attributed to the maximal ionization of the polyelectrolytes in the mixture. After 30 minutes of complexation, macroscopic phase separation was observed only for stoichiometric complexation ( $n^-/n^+ = 1$ ), characterized by a coexistence of small precipitates and a clear supernatant (**Figure 3**). Meanwhile, all other  $n^-/n^+$  led to the formation of visually homogeneous systems, changing from clear to turbid dispersions as  $n^-/n^+$  was closer to stoichiometric value. Only such homogeneous samples were subjected to particle size and zeta potential measurements. As shown in **Figure 4A**, the non-stoichiometric complexation between  $HA_M$  and DEAE-D formed nanoparticles with

mean  $D_h$  in the range of 150-350 nm. As  $n/n+$  approached the unity, the particle sizes decreased, along with narrower size distributions and lower absolute values of zeta potential (Figure 4A-B).

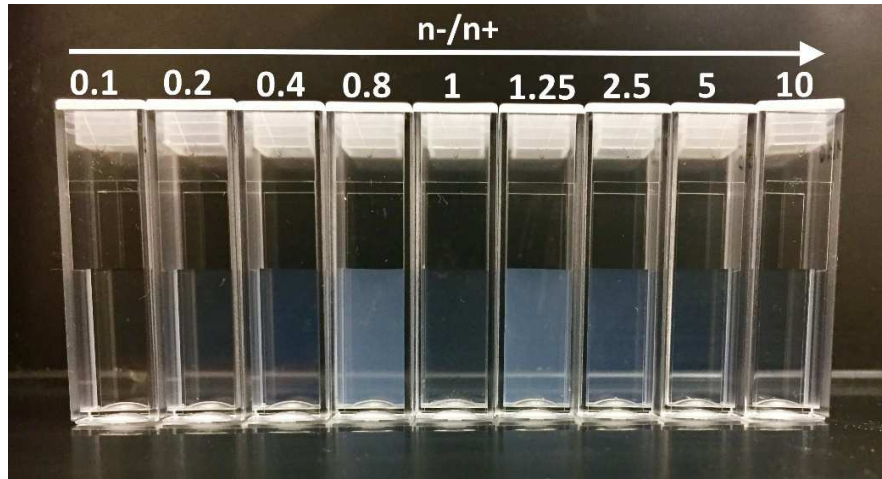


**Figure 3.** Visual aspect of  $HA_M/DEAE-D$  PECs in function of  $n/n+$  at  $C_P = 0.5 \text{ g.L}^{-1}$  in Milli-Q water at different  $n/n+$  after 30 minutes of complexation under stirring

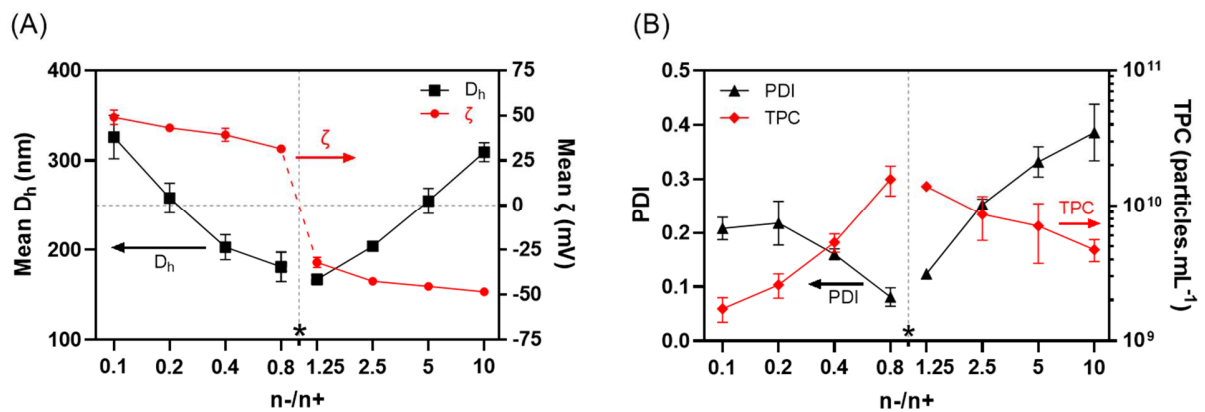


**Figure 4.** (A) Mean hydrodynamic diameter and mean zeta potential, (B) polydispersity index and total particle concentration (TPC) of  $HA_M/DEAE-D$  PECs at  $C_P = 0.5 \text{ g.L}^{-1}$  in Milli-Q water at different  $n/n+$  after 30 minutes of complexation under stirring. Asterisks denote precipitation at  $n/n+ = 1$ . Error bars represent mean  $\pm$  standard deviation ( $n \geq 3$ ).

In the literature, relatively similar tendencies in particle size (i.e. lower particle size at charge ratio nearer to 1) were also observed for chitosan/dextran sulfate PECs by Schatz *et al.* [8] and poly[2-(dimethylamino)ethyl methacrylate]/polyphosphate PECs by Kabanov and Zezin [33].

Such tendencies might be explained based on the model of PEC particles as secondary complexes shown in **Figure 1** as followings. At non-stoichiometric mixing ratio, ion-pairing between polyanions and polycations would lead to the formation of primary complexes comprising neutral double-stranded complexed segments and polar single-stranded segments of uncomplexed polyelectrolytes [8, 33]. Hydrophobic interactions and self-assembly of neutralized complexed segments could occur due to their potential nonpolar characteristic and might be enhanced by the presence of ethyl groups in uncharged DEAE groups, which are also known to have slightly hydrophobic property [34]. The segregation of such nonpolar segments *via* hydrophobic interactions with other interactions (i.e. van der Waals forces and hydrogen bonding) would form final PECs particles as secondary complexes comprising relatively hydrophobic cores surrounded by hydrophilic corona shells of polar uncomplexed polyelectrolyte segments [3, 4, 8, 35, 36]. Although the core-shell model has been widely used to describe PEC-based colloidal particles, the work of Raik *et al.* which studied PECs from HA and diethylaminoethyl chitosan by structure factor analysis suggested PEC particles not following this model [37]. Furthermore, Zhang and Shklovskii suggested other structural models for non-stoichiometric PECs, for example intercomplex disproportionation in which there is a coexistence of macroscopic neutral droplets and highly charged soluble PECs, and intracomplex disproportionation in which PECs are described as “tadpoles” having one end as neutral complex in the form of condensed droplet and the other end as highly charged tail [38]. However, in our work, the high zeta potential which decreases when  $n^-/n^+$  is nearer to 1 (**Figure 4**) with accordingly decreased  $I_I/I_{III}$  in the pyrene fluorescence spectra (see section 3.3) seem to suggest the copresence of highly charged and hydrophilic outer shell and a relatively more hydrophobic core respectively in HA/DEAE-D particles. Based on this presumption, a  $n^-/n^+$  ratio closer to 1

probably generates particles having thinner and less polar shells with more hydrophobic cores due to more efficacious charge neutralization, leading to a more compact structure (i.e. smaller size) of the final particles. This trend was also observed at other polymer concentrations (i.e.  $C_P = 0.3$  and  $1 \text{ g.L}^{-1}$ ) as mentioned in section 3.1.2.

At the stoichiometric charge ratio, the charge compensation was probably complete, as seen with the zeta potential (net surface charge) around zero (**Figure 4A**). This could favour aggregation and explained the observed precipitation. One should also notice that particle size of PECs can abruptly increase at  $n^-/n^+$  very close to the unity due to particle aggregation when charge compensation is nearly complete [8]. However, this was not observed in the current work as  $n^-/n^+$  at 0.8 and 1.25 might not be extremely close to 1 for such phenomenon to be visible. Despite the smaller particle size, the turbidity become more pronounced for these samples, which should be attributed to the increase in particle concentration (**Figure 4B**) as also described in the literature [8]. It should be noticed that high turbidity might lead to multiple light scattering which could affect particle size analysis [39]. However, for the systems in this work, the turbidity was not extremely high and the mass concentrations of the studied samples were rather low ( $0.3\text{-}1 \text{ g.L}^{-1}$ , which means  $0.03\text{-}0.1 \%$  m/v) in comparison with the high concentrations at which multiple light scattering showing major effect as described in the literature, for example  $8 \text{ g.L}^{-1}$  or  $10\%$  m/v for some protein-based colloidal systems [39]. Furthermore, the Malvern Zetasizer Ultra in this work uses the Non-Invasive Backscatter technique allowing automatic optimization of measurement position to avoid multiple light scattering effect and the attenuator index in the particle size analysis results was not too low (5 to 7) with resulting mean count rates of 200-500 kcps, which suggest acceptable concentrations [40]. For these reasons, the multiple light scattering is likely to have little effect on our particle size results.

### 3.1.2. Influence of total polymer concentration

To evaluate the impact of total polymer concentration ( $C_P$ ), HA<sub>M</sub>/DEAE-D PECs with n-/n+ from 0.1 to 10 were prepared and studied for  $C_P$  of 0.3, 0.5 (section 3.1.1) and 1 g.L<sup>-1</sup> in Milli-Q water. As for  $C_P = 0.5$  g.L<sup>-1</sup>, the stoichiometric mixing at  $C_P$  of 0.3 and 1 g.L<sup>-1</sup> also led to visible precipitation. The DLS results of PECs at other n-/n+ showed that larger particles with larger size distributions were formed as  $C_P$  was increased from 0.3 to 1 g.L<sup>-1</sup> (**Figure 5A-B**). However, the trends of  $D_h$  and PDI in function n-/n+ are the same for all studied  $C_P$  i.e. lower mean  $D_h$  and PDI at n-/n+ nearer to 1 as described in section 3.1.1.

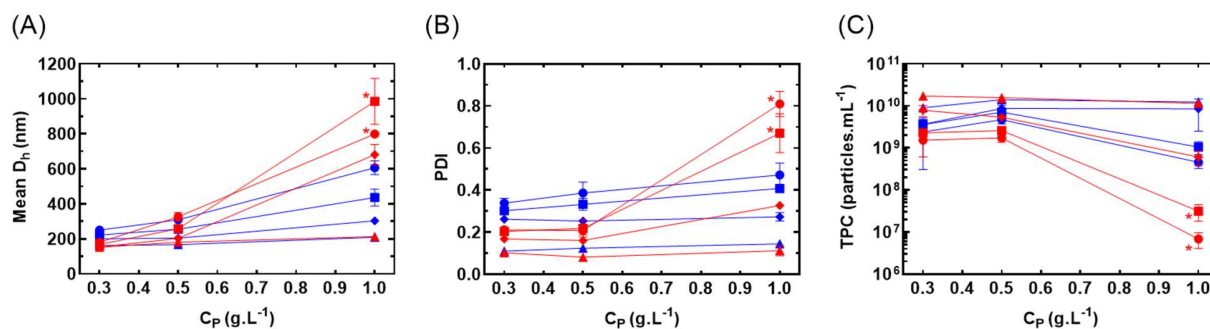


**Figure 5.** (A) Mean hydrodynamic diameter, (B) polydispersity index and (C) total particle concentration of HA<sub>M</sub>/DEAE-D PECs in Milli-Q water as a function of total polymer concentration at different n-/n+ ratios: 0.1 (—●—), 0.2 (—■—), 0.4 (—◆—), 0.8 (—▲—), 1.25 (—▲—), 2.5 (—◆—), 5 (—■—), 10 (—●—). Asterisks denote samples having highly heterogeneous multimodal particle size distribution with poor repeatability. Error bars represent mean  $\pm$  standard deviation ( $n \geq 3$ ).

The larger PEC particles observed at higher  $C_P$  for all n-/n+ were probably due to a higher amount of associated polymer in the particles. According to Müller *et al.*, as final particles of PECs are secondary particles formed by the aggregation of primary PECs, the increase in  $C_P$  would reduce the Debye length of the system and in turn lead to a reduction in the repulsion between primary PECs, which favours the formation of bigger secondary PECs [36]. The increase range in particle size was less important at n-/n+ near 1, presumably due to the more

compact structure of PECs at such charge ratios. In accordance with the increasing particle size, we observed higher turbidity of PEC suspensions at higher  $C_P$  for the same  $n-/n+$  (results not shown). Hence, the turbidity in this case seemed to be dependent on particle size, but not necessarily on particle number since the amounts of particles were not greatly changed (for  $n-/n+ \geq 0.4$ ) or even decreased (for  $n-/n+$  of 0.1 and 0.2) with increased  $C_P$  (**Figure 5C**).

Furthermore, at  $C_P = 1 \text{ g.L}^{-1}$ , remarkably high mean  $D_h$  with multimodal size distribution and very high PDI ( $\text{PDI} > 0.5$ ) at low values of  $n-/n+$  (i.e. 0.1 and 0.2) coincided with significant low TPC. These results seem to indicate fewer but larger particles uncontrolled in size. This could be explained again from the model of PECs shown in **Figure 1**. In case of very low  $n-/n+$ , the neutral segments in primary PECs are much shorter than those at high  $n-/n+$ , which would consequently require a very high number of primary PECs involved to form sufficiently stable cores in secondary particles, leading to much fewer final particles with much larger size. Such high particle size can also be attributed to the loose structure of the core due to weaker hydrophobic interactions of shorter neutral complexed segments [6]. Besides the core, the particle size should also be greatly governed by the thickness of their shell, which is directly related to the chain length (contour length) of the polyelectrolyte in excess [6]. This assumption could also explain the larger particle size for  $\text{HA}_M/\text{DEAE-D}$  PECs at very low  $n-/n+$  compared with high  $n-/n+$  since the corona shell in the former case was formed by long segments of uncomplexed DEAE-D, which had a higher chain length than that of  $\text{HA}_M$ . Such difference in particle size between the two extremities of the  $n-/n+$  range seemed to be only significant at  $C_P = 1 \text{ g.L}^{-1}$ . In case of  $C_P = 0.5 \text{ g.L}^{-1}$ , this was not observed after 30 minutes of complexation but became evident after 24 h (see Section 3.2.1). This was possibly because lower  $C_P$  led to weaker

interchain and intercomplex interactions within the PEC suspension, resulting in slower kinetics of the systems to reach their equilibrium state.

### 3.1.3. Influence of molar mass

In order to evaluate the impact of polyelectrolyte molar mass on PECs formation, HA<sub>H</sub>/DEAE-D PECs were compared with HA<sub>M</sub>/DEAE-D at identical n-/n+ and C<sub>P</sub> (n-/n+ = 0.1-10 and C<sub>P</sub> of 0.3 and 0.5 g.L<sup>-1</sup>). At C<sub>P</sub> = 0.5 g.L<sup>-1</sup>, the complexation between HA<sub>H</sub> and DEAE-D consistently led to precipitation in the whole studied range of n-/n+. Upon decreasing C<sub>P</sub> to 0.3 g.L<sup>-1</sup>, the precipitation was less intense and not observed at n-/n+ of 0.1 and 10. As can be seen from the particle size measurements of these samples (**Figure 6**), complexation between DEAE-D and HA of higher molar mass led to PECs with higher diameter and PDI but TPC not significantly changed. A similar observation reported by Schatz *et al.* also showed an increase in PEC particle size after increasing the molar mass of chitosan (from  $0.13 \times 10^5$  to  $3.65 \times 10^5$  g.mol<sup>-1</sup>) for complexation with dextran sulfate of fixed molar mass ( $5 \times 10^5$  g.mol<sup>-1</sup>) [8]. Müller *et al.* also reported increasing particle size of PEI/polyacrylic acid PECs resulting from the increase in molar mass of the two associating polyelectrolytes [36].

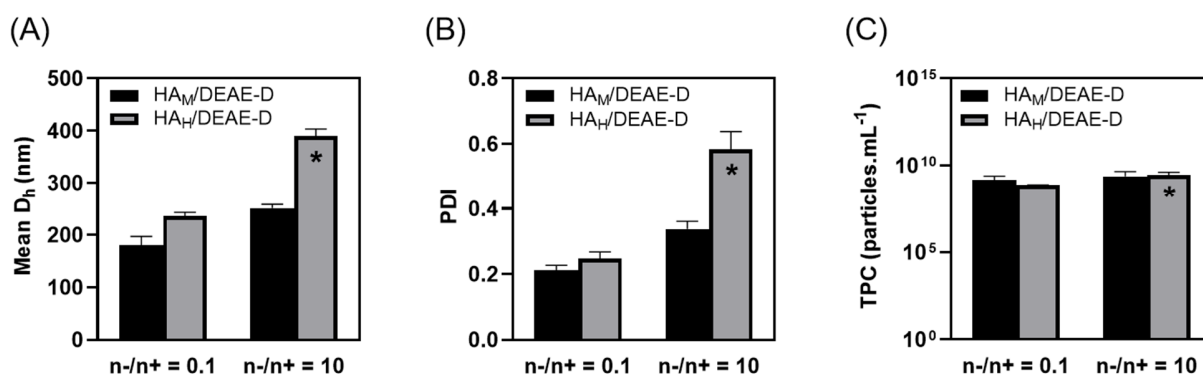


**Figure 6.** (A) Mean hydrodynamic diameter, (B) polydispersity index and (C) total particle concentration of HA<sub>M</sub>/DEAE-D and HA<sub>H</sub>/DEAE-D PECs at C<sub>P</sub> = 0.3 g.L<sup>-1</sup> in Milli-Q water at n-/n+ of 0.1 and 10. Asterisks denote samples having highly heterogeneous multimodal particle size distributions with poor repeatability. Error bars represent mean ± standard deviation (n ≥ 3).

In the current work, while DEAE-D is a flexible polysaccharide with mainly  $\alpha(1\rightarrow6)$  glycosidic linkages, HA is relatively stiffer with less flexible  $\beta(1\rightarrow4)$  and  $\beta(1\rightarrow3)$  glycosidic bonds [41, 42]. This can also be seen from the expanding coil structure of HA shown by its high  $R_g$  values in **Table 1**. As a result, a HA chain length which was higher and closer to that of DEAE-D would certainly lead to the formation of longer and more rigid neutralized segments in primary complexes compared with medium molar mass HA, which could favour the aggregation to form larger secondary particles and hence the macroscopic phase separation. In the case of  $n-/n+ > 1$ , the observed increase in particle size could also be attributed to the increased thickness of the particle shells due the presence of higher chain length and more expanding hydrodynamic coil structure of  $HA_H$  compared with  $HA_M$ . All these synergistic effects probably explain the more obvious increase in PEC size at  $n-/n+ = 10$  than at  $n-/n+ = 0.1$ . Furthermore, at  $n-/n+ = 10$ , the  $D_h$  distribution of  $HA_H/DEAE-D$  PECs was multimodal and heterogeneous. This might result from the high viscosity of the bulk phase due to the excessive presence and the long chain length of  $HA_H$ , preventing the homogeneous distribution of DEAE-D to form same-sized particles.

#### 3.1.4. Influence of ionic strength

The effect of ionic strength on PECs formation was studied by characterizing  $HA_M/DEAE-D$  PECs ( $C_P = 0.5 \text{ g.L}^{-1}$ ) and  $HA_H/DEAE-D$  PECs ( $C_P = 0.3 \text{ g.L}^{-1}$ ) at  $n-/n+$  from 0.1 to 10 prepared at NaCl concentration ( $[NaCl]$  varying from 0 to  $1 \text{ mol.L}^{-1}$ ). After the complexation, samples showing precipitation are reported in **Table 2**. The presence of NaCl seemed to have a non-monotonic influence on PECs depending on its concentration: (i) reducing the formation of PECs at low salt concentration ( $10^{-3} \text{ mol.L}^{-1}$ ), (ii) favouring PECs aggregation as well as macroscopic phase separation at intermediate salt concentration ( $10^{-2}$  -  $10^{-1} \text{ mol.L}^{-1}$ ) and (iii) depress the complexation at very high salt concentration ( $1 \text{ mol.L}^{-1}$ ). For  $HA_M/DEAE-D$  PECs ( $C_P = 0.5$

g.L<sup>-1</sup>), the initial n-/n+ range of precipitation might be too narrow for the reduction of precipitation at low salt concentration to be visible. The last two effects of salt on the phase behaviour (i.e. increase followed by suppression of phase separation) were also described for other PECs systems [38, 43]. This may result from the fact that associative phase separation (caused by ion pairing) and segregative phase separation (caused by hydrogen bonding and hydrophobic interactions) are respectively reduced and enhanced with added salt [44]. In order to clarify such effects of salt on our specific system, particle size characterization by DLS were conducted for the HA<sub>M</sub>/DEAE-D PECs (C<sub>P</sub> = 0.5 g.L<sup>-1</sup>) samples at n-/n+ = 0.2 and 5 within the studied range of salt concentration (**Figure 7**).

**Table 2.** Visual aspect of HA/DEAE-D PEC dispersions at various NaCl concentration

	[NaCl] (mol.L <sup>-1</sup> )	n-/n+								
		0.1	0.2	0.4	0.8	1	1.25	2.5	5	10
HA <sub>M</sub> /DEAE-D C <sub>P</sub> = 0.5 g.L <sup>-1</sup>	0	-	-	-	-	+	-	-	-	-
	1 × 10 <sup>-3</sup>	-	-	-	-	+	-	-	-	-
	1 × 10 <sup>-2</sup>	-	-	-	+	+	+	-	-	-
	1 × 10 <sup>-1</sup>	-	-	+	+	+	+	+	-	-
	1	-	-	-	-	-	-	-	-	-
	0	-	+	+	+	+	+	+	+	-
HA <sub>H</sub> /DEAE-D C <sub>P</sub> = 0.3 g.L <sup>-1</sup>	5 × 10 <sup>-4</sup>	-	-	-	+	+	-	-	-	-
	1 × 10 <sup>-3</sup>	-	-	-	-	+	-	-	-	-
	5 × 10 <sup>-3</sup>	-	-	-	-	+	+	-	-	-
	1 × 10 <sup>-2</sup>	-	-	-	+	+	+	-	-	-
	1 × 10 <sup>-1</sup>	-	-	+	+	+	+	-	-	-
	1	-	-	-	-	-	-	-	-	-

: precipitation; -: homogeneous samples

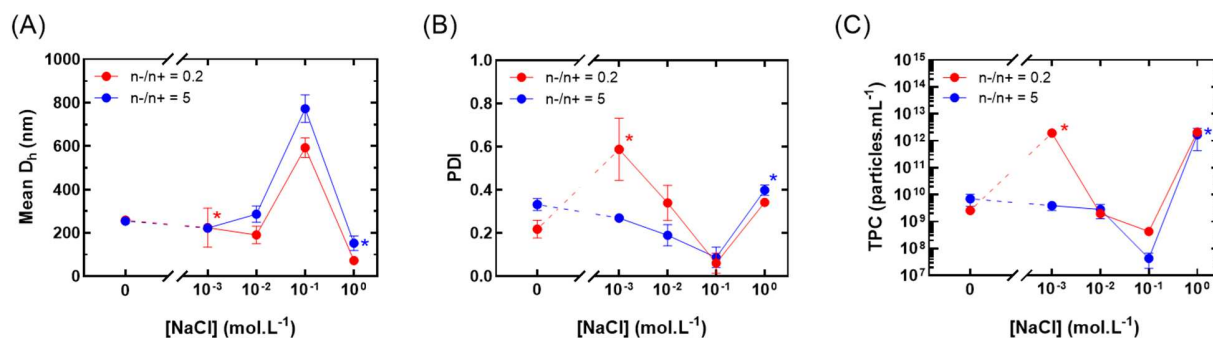


**Figure 7.** (A) Mean hydrodynamic diameter, (B) polydispersity index and (C) total particle concentration of HA<sub>M</sub>/DEAE-D PECs ( $C_P = 0.5 \text{ g.L}^{-1}$ ) of  $n-/n+ = 0.2$  and 5 prepared at different NaCl concentrations. Asterisks denote samples having highly heterogeneous multimodal particle size distributions with poor repeatability. Error bars represent mean  $\pm$  standard deviation ( $n \geq 3$ ).

The suggested effects of ionic strength can be clearly seen from the results obtained with the samples having  $n-/n+ = 0.2$ . At  $[\text{NaCl}] = 10^{-3} \text{ mol.L}^{-1}$ , the PECs particle size became poorly defined with its distribution being highly heterogeneous with remarkably high TPC, probably due to the formation of loosely structured PECs with some small-sized particle populations, possibly because the primary complexation is rendered less effective by charge screening at macromolecular level. However, this effect seems to be hindered for PECs of  $n-/n+ = 5$ , possibly due to the more stable structure of these PECs (sections 3.1.2 and 3.2). Anyway, when  $[\text{NaCl}]$  is higher than  $10^{-3} \text{ mol.L}^{-1}$ , effects of salt on PECs seem to be similar for both  $n-/n+$  ratios: less particles were counted while the particle size distributions were narrower, but the mean  $D_h$  was increased to more than 500 nm as the salt concentration reached  $10^{-1} \text{ mol.L}^{-1}$ , indicating the formation of fewer but larger particles in accordance with the observed increase in precipitation at other  $n-/n+$  between 0.2 and 5. This may be due to higher aggregation of PECs because of more efficacious hydrophobic interactions and weaker electrostatic repulsion caused by charge screening at complex and particle level. Specifically, the mean  $D_h$  at  $n-/n+ = 0.2$  was better defined with less variation than at  $[\text{NaCl}] = 10^{-3} \text{ mol.L}^{-1}$ . Therefore, intermediate salt

concentration seems to favour secondary complexation in compensation for the weakened primary complexation, leading to a stabilizing effect to form more close-packed and homogeneous PECs. These two opposing effects of salt on PEC particle size were also reported for sodium polystyrene sulfonate/poly(diallyldimethylammonium chloride) PECs by Dautzenberg *et al.* [45]. However, when the salt concentration was extremely high (1 mol.L<sup>-1</sup>), the charged groups of the two polyelectrolytes were almost completely screened from the beginning and the complexation was almost ineffective, leading to the clear aspect of all PEC suspensions even at  $n/n+ = 1$ . This was also shown by the abrupt fall of particle sizes with very high particle concentration. It should be noticed that the critical salt concentration needed to completely suppress the complexation may vary depending not only on the type of polyelectrolytes but also on their concentration and pH in the system [43, 44].

### 3.1.5. Influence of mixing order and mixing mode

To study the influence of mixing mode and mixing order, PECs of HA<sub>M</sub>/DEAE-D in Milli-Q water at  $C_P = 0.5 \text{ g.L}^{-1}$  and  $n/n+$  of 0.1, 0.8, 1.25 and 10 were prepared by either one-shot addition using a micropipette or dropwise addition (0.3 mL.min<sup>-1</sup>) using a syringe pump in both addition orders. The impact of these two parameters on PECs formation was evaluated by comparing the mean particle sizes of PECs prepared by different methods (**Figure 8**).

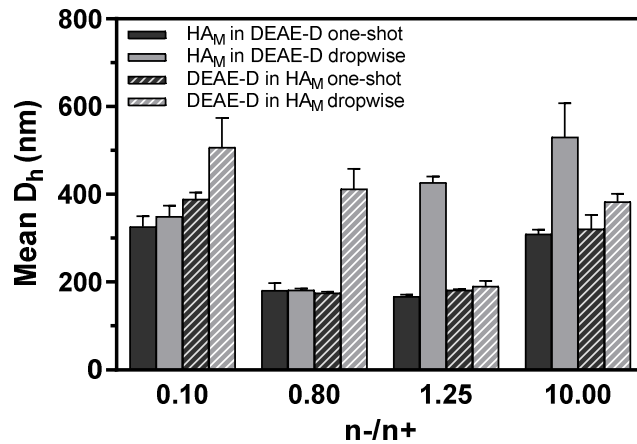


**Figure 8.** Mean hydrodynamic diameter of HA<sub>M</sub>/DEAE-D PECs in Milli-Q water at  $C_P = 0.5 \text{ g.L}^{-1}$  prepared with different mixing orders and mixing modes. Error bars represent mean  $\pm$  standard deviation ( $n \geq 3$ ).

As can be seen from the results, the effect of mixing order on mean particle size was negligible in one-shot mode but became considerable when PECs were prepared by dropwise mixing. At any n-/n+ ratio, remarkably large particle sizes were only observed when the polyelectrolyte in excess was added dropwise to the other polyelectrolyte, while the other three mixing methods resulted to lower and similar particle sizes. The distinct result in the former case could be explained based on the actual evolution of n-/n+ during the mixing, which was also described by Schatz *et al.* [6] and Raik *et al.* [37]. In this case, on adding slowly excess HA to default DEAE-D or excess DEAE-D to default HA, the actual n-/n+ of the mixture would evolve from 0 to more than 1 or from  $+\infty$  to less than 1, respectively. Large aggregates could hence be formed due to complete charge neutralization as n-/n+ passed over 1 as the dropping speed was sufficiently low compared with the aggregation kinetics [37]. The large aggregates remained even at extreme final n-/n+ (0.1 and 10), meaning that such aggregation was apparently irreversible. In case of one-shot addition, such effect was hindered since the n-/n+ changed so rapidly that the aggregation did not have enough time to occur and hence the particle sizes were lower and did

not show significant difference between the two orders of addition. In case of adding the default polyelectrolyte to the excess polyelectrolyte, the particle sizes were not considerably different between the two modes of mixing at whichever  $n-/n+$ , indicating the addition speed does not have great influence on PEC particle size in such cases.

### **3.2. Stability of PECs**

#### *3.2.1. Effect of charge ratio and storage temperature*

In order to investigate the stability of HA/DEAE-D PECs, particle size of  $HA_M/DEAE-D$  PECs in Milli-Q water at  $C_P = 0.5 \text{ g.L}^{-1}$  and  $n-/n+ = 0.1-10$  were reevaluated after 1, 3, 7 and 30 days of conservation at 25 °C or 4 °C . PECs at  $n-/n+ = 1$  were not studied due the macroscopic phase separation from the beginning. For the other PECs, stability monitoring was ceased when the samples started to show highly heterogeneous particle size distribution. As can be seen from the obtained results (**Figure 9**), PECs of low  $n-/n+$  ratios ( $n-/n+ = 0.1-0.2$ ) showed increasing particle size with larger and heterogeneous particle size distribution after one day regardless of storage temperature. PECs at  $n-/n+ = 0.4$  showed a quite similar tendency but to a lesser extent, whereas PECs at  $n-/n+ \geq 0.8$  had mean particle size and PDI minorly changed after one month. The very high  $D_h$  and PDI after one day of PECs at low  $n-/n+$  should not be taken as their precise characteristics because DLS measurements are less reliable when  $D_h$  approaches 1000 nm and beyond. However, such results evidenced that  $HA_M/DEAE-D$  PECs were totally instable at such low  $n-/n+$  and storage temperature did not have significant effect on their stability. The observed lack of stability can be once again explained by the weaker hydrophobic interactions of neutral complexed blocks in primary PECs due to their lower length. To compensate this effect, the final PECs should involve more primary PECs and optimize their conformation over time to reach their equilibrium state, which could be even practically unreachable after one day. Such

aggregation was also confirmed by the decrease in particle concentration after one day as shown in **Figure 10A**.

### 3.2.2. *Effect of ionic strength and total polymer concentration*

In order to evaluate the effect of ionic strength on the stability of HA<sub>M</sub>/DEAE-D PECs at low  $n^-/n^+$ , the stability studies were also done for samples of such PECs at  $C_P = 0.5 \text{ g.L}^{-1}$  in presence of salt that have homogeneous particle size and initial mean  $D_h < 400 \text{ nm}$ , namely samples having  $n^-/n^+ = 0.1$  in NaCl  $0.1 \text{ mol.L}^{-1}$  and  $n^-/n^+ = 0.2-0.4$  in NaCl  $0.01 \text{ mol.L}^{-1}$ . As shown in **Figure 10B**, the stability of HA<sub>M</sub>/DEAE-D PECs at  $C_P = 0.5 \text{ g.L}^{-1}$  was obviously improved in NaCl  $0.01-0.1 \text{ mol.L}^{-1}$ . Particularly, the particle size of PECs at  $n^-/n^+ = 0.1$  in NaCl  $0.1 \text{ mol.L}^{-1}$  increased during the first three days but the range of increase was less considerable than the previous results and the particle size distribution was always homogeneous. For PECs at  $n^-/n^+$  of 0.2 and 0.4 in NaCl  $0.01 \text{ mol.L}^{-1}$ , the particle sizes were relatively stable after 7 days. This improvement of stability could be attributed to the stabilizing effect of salt at intermediate concentration as described in section 3.1.4.

In order to assess the importance of  $C_P$  in PECs stability, HA<sub>M</sub>/DEAE-D at lower  $C_P$  ( $C_P = 0.3 \text{ g.L}^{-1}$ ) for  $n^-/n^+ = 0.1$  in Milli Q water were also studied. As shown in **Figure 10B**, the particle size of this sample seemed not to significantly change after 7 days of storage, indicating a higher physicochemical stability at lower  $C_P$ . The mechanism of this phenomenon, however, remained unclear. The only possible explanation should be the presence of fewer complexes leading to less intercomplex interactions and hence lower aggregation rate.

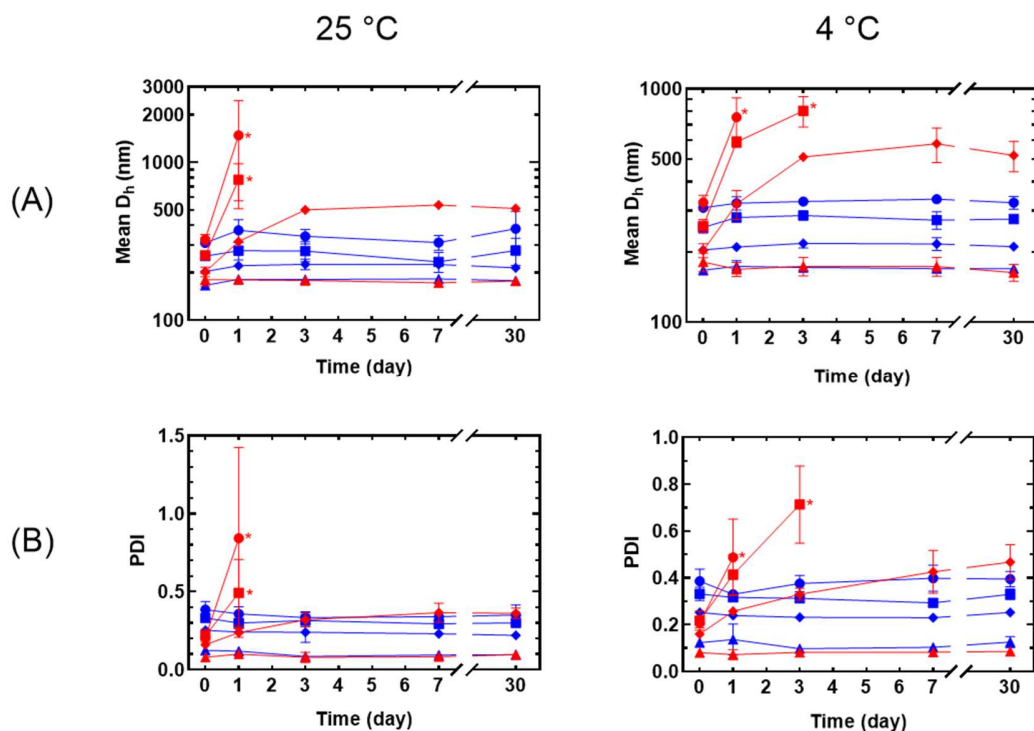


**Figure 9.** (A) Mean hydrodynamic diameter and (B) polydispersity index of  $HA_M/DEAE-D$  PECs ( $C_P = 0.5 \text{ g.L}^{-1}$ ) in Milli-Q water at different n-/n+ ratios: 0.1 (—●—), 0.2 (—■—), 0.4 (—◆—), 0.8 (—▲—), 1.25 (—▲—), 2.5 (—◆—), 5 (—■—), 10 (—●—) stored at 25 °C and 4 °C in function of storage time. Asterisks denote samples having highly heterogeneous multimodal particle size distributions with poor repeatability. Error bars represent mean  $\pm$  standard deviation (n  $\geq$  3).

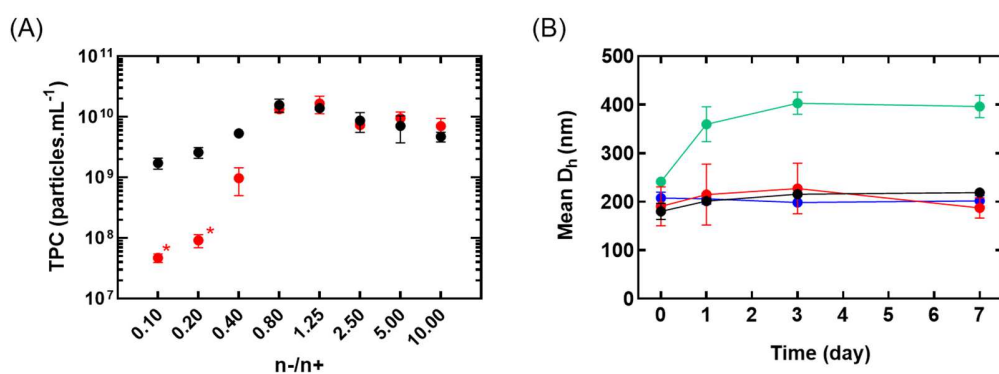


**Figure 10.** (A) Total particle concentration of  $HA_M/DEAE-D$  PECs ( $C_P = 0.5 \text{ g.L}^{-1}$ ) in Milli-Q water at different n-/n+ ratios after 30 min of complexation (●) and one day after storage at 4 °C (●). Asterisks denote samples having multimodal and heterogeneous particle size distribution. Otherwise size distributions are adequately homogeneous and unimodal. (B) Mean hydrodynamic diameter of  $HA_M/DEAE-D$  PECs at  $C_P = 0.5 \text{ g.L}^{-1}$  and n-/n+ = 0.1 - [NaCl] = 0.1 mol.L<sup>-1</sup> (—●—), n-/n+ = 0.2 - [NaCl] = 0.1 mol.L<sup>-1</sup> (—●—).

0.01 mol.L<sup>-1</sup> (●-), n-/n+ = 0.4 – [NaCl] = 0.01 mol.L<sup>-1</sup> (●-) and C<sub>P</sub> = 0.3 g.L<sup>-1</sup>, n-/n+ = 0.1 in Milli-Q water (●-) stored at 4 °C as a function of storage time. Error bars represent mean ± standard deviation (n ≥ 3).

### 3.3. Pyrene fluorescence

In this work, the fluorescence of pyrene incorporated in HA<sub>M</sub>/DEAE-D PECs was characterized in order to evaluate the relative hydrophobicity of these PECs since pyrene has its fluorescence spectra changed according to microenvironmental polarity: the presence of more hydrophobic or less hydrophilic nanodomains normally lead to a lower I<sub>I</sub>/I<sub>III</sub> ratio in its emission spectra and a higher I<sub>335</sub>/I<sub>338</sub> in its excitation spectra [29-32]. As presented in **Figure 11A**, pyrene in HA<sub>M</sub>/DEAE-D samples at n-/n+ closer to the unity had lower I<sub>I</sub>/I<sub>III</sub> in the emission spectra and higher I<sub>335</sub>/I<sub>338</sub> in the excitation spectra, compared with reference values in Milli-Q water without PECs (I<sub>I</sub>/I<sub>III</sub> = 1.894 ± 0.017 and I<sub>335</sub>/I<sub>338</sub> = 0.370 ± 0.012). The exceptional values at n-/n+ = 1 were certainly caused by the precipitation which separated PECs from the bulk phase. These results suggest the formation of slightly less hydrophilic or more hydrophobic nanodomains in PECs following charge neutralization.

However, the formation of such hydrophobic nanodomains might also be attributed to hydrophobic interactions of some DEAE groups possibly remaining deprotonated [34]. To verify this, the pyrene fluorescence characterization was also performed for PECs with the same C<sub>P</sub> and C<sub>Py</sub> from HA<sub>M</sub> and PEI, a highly hydrophilic polycation without DEAE groups. For this experiment, the pHs of the reacting solutions were adjusted to 2.9 with HCl or NaOH 0.1-1 mol.L<sup>-1</sup> before their complexation because (i) the pH of freshly prepared PEI hydrochloride solution was readily around 2.9 and (ii) this pH could ensure the complete protonation of PEI, otherwise at any higher pH its ionization rate could not be straightforward estimated as for HA

[46]. For  $n^-/n^+$  calculation, the  $\alpha$  values of HA and PEI at  $\text{pH} = 2.9$  were 0.5 and 1 respectively and  $M_0$  of PEI was  $43 \text{ g}\cdot\text{mol}^{-1}$ . As can be seen from **Figure 11B**,  $\text{HA}_M/\text{PEI}$  PECs also showed decreasing  $I_I/I_{III}$  when  $n^-/n^+$  approached 1. During this experiment, precipitation was remarked in samples at  $n^-/n^+$  from 0.8 to 1.25, which explained the unusually high  $I_I/I_{III}$  values at these charge ratios. These results confirmed the formation of hydrophobic core in PEC particles due to charge neutralization irrespective of polyelectrolyte chemical structure and that the DEAE groups did not significantly contribute to the hydrophobicity of HA/DEAE-D PECs.

To further investigate the importance of  $C_P$  and pyrene incorporation order, we also prepared  $\text{HA}_M/\text{DEAE-D}$  PECs ( $n^-/n^+ = 0.8$  and 1.25) containing pyrene by alternating  $C_P$  (0.25 and  $0.5 \text{ g}\cdot\text{L}^{-1}$ ) and preparation methods: method (a) consisted in incorporating pyrene into PECs after their formation, while in method (b) pyrene was present during the complexation. As can be seen from **Figure 11C**, changing from method (a) to method (b) led to a considerable decrease in  $I_I/I_{III}$  of pyrene fluorescence. Such results with method (b) could be attributed to the entrapment of pyrene in PECs during the complexation which resulted in a more effective incorporation of pyrene, while in method (a) the entrance of pyrene molecules into the PEC cores was disfavoured by the PEC hydrophilic shells. Meanwhile, the increase from 0.25 to  $0.5 \text{ g}\cdot\text{L}^{-1}$  in  $C_P$  led to a slight decrease of  $I_I/I_{III}$  for method (a) and almost no difference in  $I_I/I_{III}$  for method (b), probably because the presence of numerous and large PEC particles at higher  $C_P$  allowed a more efficient incorporation of pyrene to PECs in method (a) while the entrapment of readily present pyrene in PECs in the case of method (b) did not depend on this effect. In case of elaboration of PECs as a mean of drug delivery, such results with pyrene as a model molecule could contribute to the optimization of encapsulation method for hydrophobic active ingredients.

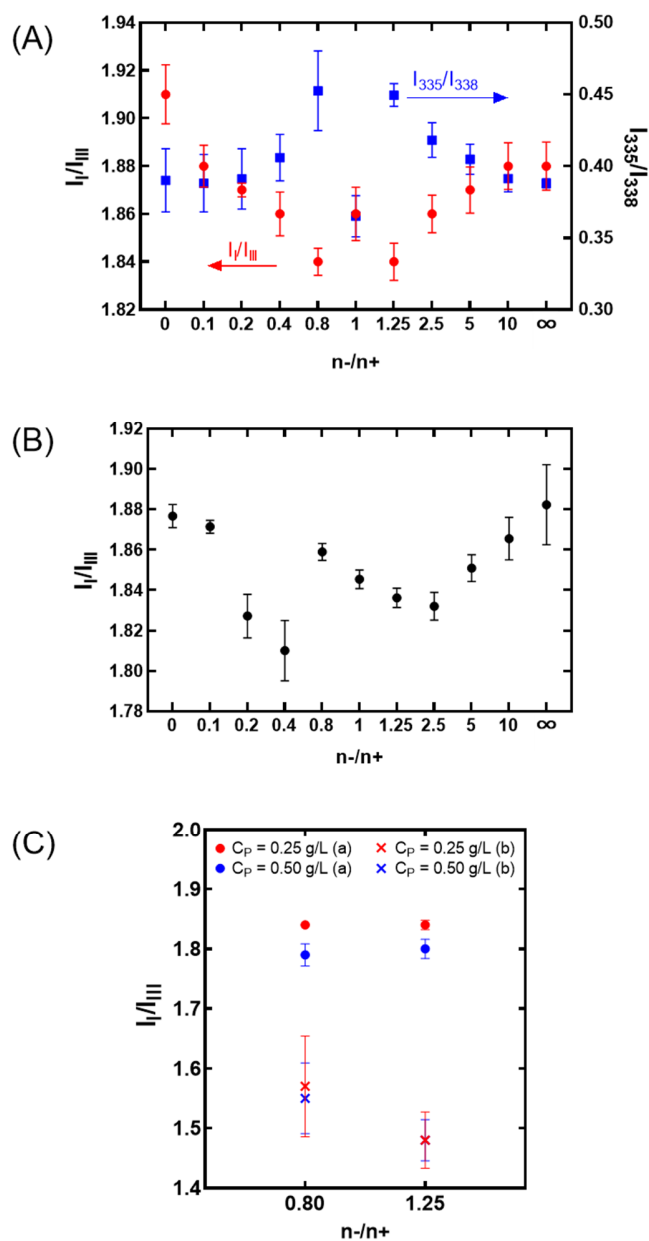


**Figure 11.** (A)  $I_I/I_{III}$  of the fluorescence emission spectra at  $\lambda_{ex} = 335$  nm and  $I_{335}/I_{338}$  of the fluorescence excitation spectra of  $\lambda_{em} = 373$  nm of  $HA_M/DEAE-D/Py$  in Milli-Q water at  $C_P = 0.25$  g.L<sup>-1</sup> and  $C_{Py} = 4 \times 10^{-7}$  mol.L<sup>-1</sup> prepared with method (a) in function of  $n-/n+$ . (B)  $I_I/I_{III}$  of the fluorescence emission spectra at  $\lambda_{ex} = 335$  nm of  $HA_M/PEI/Py$  in Milli-Q water at  $C_P = 0.25$  g.L<sup>-1</sup> and  $C_{Py} = 4 \times 10^{-7}$  mol.L<sup>-1</sup> prepared with method (a) in function of  $n-/n+$ . The values 0 and  $\infty$  of  $n-/n+$  correspond respectively to the aqueous solutions of DEAE-D and  $HA_M$  containing pyrene. (C)  $I_I/I_{III}$  of the fluorescence emission spectra at  $\lambda_{ex} = 335$  nm of  $HA_M/DEAE-D/Py$  in Milli-Q water at  $n-/n+ = 0.8$  and  $1.25$ ,  $C_{Py} = 4 \times 10^{-7}$  mol.L<sup>-1</sup>,  $C_P = 0.25$  and  $0.5$  g.L<sup>-1</sup>, prepared with methods (a) and (b). Error bars represent mean  $\pm$  standard deviation ( $n \geq 3$ ).

#### **4. Conclusion**

In this work, the influences of charge ratio, total polymer concentration, polymer molar mass, ionic strength, mixing order and mixing mode on the formation of HA/DEAE-D PECs were investigated. When the  $n^-/n^+$  approached the unity, PECs had more compact and relatively more hydrophobic structure with lower particle size, while phase separation occurred following stoichiometric mixing due to optimum charge neutralization. Higher polymer concentration generally led to larger PEC particles. The employment of HA having higher molar mass also resulted in higher particle size. Unlike these factors, the influence of ionic strength was non-monotonic as a compromise between limiting effect and enhancement effect on PEC formation, due to charge screening at macromolecular level and particle level respectively. The effect of mixing order and mixing mode were interdependent and depended also on  $n^-/n^+$ , with larger PECs being formed in case of adding dropwise the polyelectrolyte in excess to the other. Furthermore, the physicochemical stability of HA/DEAE-D PECs during storage was proved to be strongly dependent on  $n^-/n^+$  and can be improved by increasing ionic strength or decreasing polymer concentration. The pyrene fluorescence studies also confirmed the relatively hydrophobic core in PECs resulting from charge neutralization. The addition of pyrene prior to polyelectrolyte complexation also led to a more efficacious incorporation of pyrene in PECs. In the context of drug delivery, such results suggested a promising conception for efficient encapsulation and delivery of hydrophobic active molecules. To that end, further studies are also ongoing based on HA/DEAE-D as a low-cost model system to understand and optimize PEC systems for therapeutic applications.

#### **Acknowledgments**

We thank the Normandy region and the European Union for their financial support.

### **Authors' Contributions**

**Huu Van LE:** Conceptualization, Investigation, Writing- Original Draft preparation. **Virginie DULONG:** Investigation, Validation, Writing- Reviewing and Editing. **Luc PICTON:** Methodology, Writing- Reviewing and Editing. **Didier LE CERF:** Funding acquisition, Supervision, Writing- Reviewing and Editing, Project administration

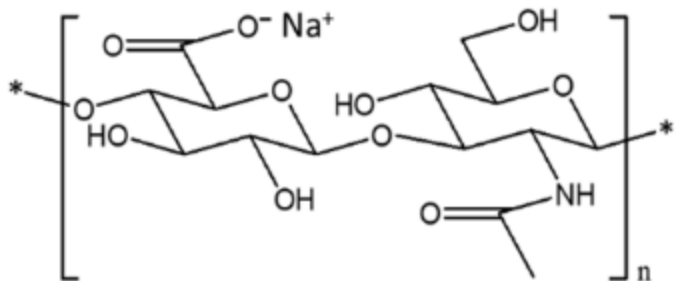
## REFERENCES

- [1] C.B. Bucur, Z. Sui, J.B. Schlenoff, Ideal mixing in polyelectrolyte complexes and multilayers: Entropy driven assembly, *J. Am. Chem. Soc.*, 128 (2006) 13690-13691. <https://doi.org/10.1021/ja064532c>.
- [2] B. Philipp, H. Dautzenberg, K.-J. Linow, J. Kötzt, W. Dawydoff, Polyelectrolyte complexes - recent developments and open problems, *Prog. Polym. Sci.*, 14 (1989) 91-172. [https://doi.org/10.1016/0079-6700\(89\)90018-X](https://doi.org/10.1016/0079-6700(89)90018-X).
- [3] S.L. Perry, L. Leon, K.Q. Hoffmann, M.J. Kade, D. Priftis, K.A. Black, D. Wong, R.A. Klein, C.F. Pierce, K.O. Margossian, Chirality-selected phase behaviour in ionic polypeptide complexes, *Nat. Commun.*, 6 (2015) 1-8. <https://doi.org/10.1038/ncomms7052>.
- [4] J. Koetz, S. Kosmella, *Polyelectrolytes and nanoparticles*, Springer Science & Business Media, Berlin, 2007.
- [5] Q. Wang, J.B. Schlenoff, The polyelectrolyte complex/coacervate continuum, *Macromolecules*, 47 (2014) 3108-3116. <https://doi.org/10.1021/ma500500q>.
- [6] C. Schatz, A. Domard, C. Viton, C. Pichot, T. Delair, Versatile and efficient formation of colloids of biopolymer-based polyelectrolyte complexes, *Biomacromolecules*, 5 (2004) 1882-1892. <https://doi.org/10.1021/bm049786>.
- [7] H. Fukuda, Y. Kikuchi, Polyelectrolyte complexes of sodium dextran sulfate with chitosan, 2, *Makromol. Chem.*, 178 (1977) 2895-2899. <https://doi.org/10.1002/macp.1977.021781012>.
- [8] C. Schatz, J.-M. Lucas, C. Viton, A. Domard, C. Pichot, T. Delair, Formation and properties of positively charged colloids based on polyelectrolyte complexes of biopolymers, *Langmuir*, 20 (2004) 7766-7778. <https://doi.org/10.1021/la049460m>.
- [9] A.D. Kulkarni, Y.H. Vanjari, K.H. Sancheti, H.M. Patel, V.S. Belgamwar, S.J. Surana, C.V. Pardeshi, Polyelectrolyte complexes: mechanisms, critical experimental aspects, and applications, *Artif. Cells, Nanomed., Biotechnol.*, 44 (2016) 1615-1625. <https://doi.org/10.3109/21691401.2015.1129624>.
- [10] A. Drogoz, L. David, C. Rochas, A. Domard, T. Delair, Polyelectrolyte complexes from polysaccharides: formation and stoichiometry monitoring, *Langmuir*, 23 (2007) 10950-10958. <https://doi.org/10.1021/la7008545>.
- [11] R. Gernandt, L. Wågberg, L. Gärdlund, H. Dautzenberg, Polyelectrolyte complexes for surface modification of wood fibres: I. Preparation and characterisation of complexes for dry and wet strength improvement of paper, *Colloids Surf., A*, 213 (2003) 15-25. [https://doi.org/10.1016/S0927-7757\(02\)00335-7](https://doi.org/10.1016/S0927-7757(02)00335-7).
- [12] C. Tan, G.B. Celli, M.J. Selig, A. Abbaspourrad, Catechin modulates the copigmentation and encapsulation of anthocyanins in polyelectrolyte complexes (PECs) for natural colorant stabilization, *Food Chem.*, 264 (2018) 342-349. <https://doi.org/10.1016/j.foodchem.2018.05.018>.
- [13] M. Ishihara, S. Kishimoto, S. Nakamura, Y. Sato, H. Hattori, Polyelectrolyte complexes of natural polymers and their biomedical applications, *Polymers*, 11 (2019) 672. <https://doi.org/10.3390/polym11040672>.
- [14] J.M. Horn, R.A. Kapelner, A.C. Obermeyer, Macro- and microphase separated protein-polyelectrolyte complexes: Design parameters and current progress, *Polymers*, 11 (2019) 578. <https://doi.org/10.3390/polym11040578>.
- [15] Y. Luo, Q. Wang, Recent development of chitosan-based polyelectrolyte complexes with natural polysaccharides for drug delivery, *Int. J. Biol. Macromol.*, 64 (2014) 353-367. <https://doi.org/10.1016/j.ijbiomac.2013.12.017>.

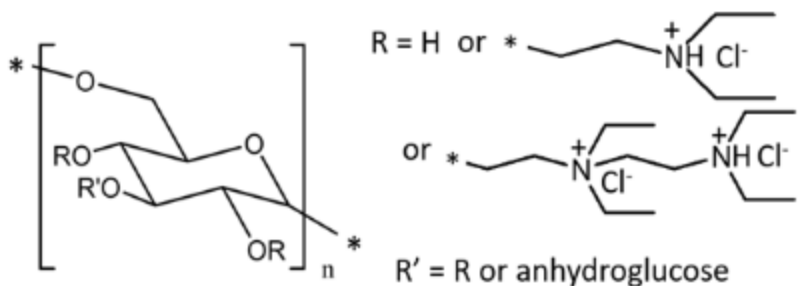
- [16] J. Necas, L. Bartosikova, P. Brauner, J. Kolar, Hyaluronic acid (hyaluronan): a review, *Vet. Med. (Prague, Czech Repub.)*, 53 (2008) 397-411. <https://doi.org/10.17221/1930-VETMED>.
- [17] G. Mattheolabakis, L. Milane, A. Singh, M.M. Amiji, Hyaluronic acid targeting of CD44 for cancer therapy: from receptor biology to nanomedicine, *J. Drug Targeting*, 23 (2015) 605-618. <https://doi.org/10.3109/1061186X.2015.1052072>.
- [18] B. Luppi, F. Bigucci, L. Mercolini, A. Musenga, M. Sorrenti, L. Catenacci, V. Zecchi, Novel mucoadhesive nasal inserts based on chitosan/hyaluronate polyelectrolyte complexes for peptide and protein delivery, *J. Pharm. Pharmacol.*, 61 (2009) 151-157. <https://doi.org/10.1211/jpp.61.02.0003>.
- [19] F. Vecchies, P. Sacco, E. Decleva, R. Menegazzi, D. Porrelli, I. Donati, G. Turco, S. Paoletti, E. Marsich, Complex coacervates between a lactose-modified chitosan and hyaluronic acid as radical-scavenging drug carriers, *Biomacromolecules*, 19 (2018) 3936-3944. <https://doi.org/10.1021/acs.biomac.8b00863>.
- [20] L. Yang, S. Gao, S. Asghar, G. Liu, J. Song, X. Wang, Q. Ping, C. Zhang, Y. Xiao, Hyaluronic acid/chitosan nanoparticles for delivery of curcuminoid and its in vitro evaluation in glioma cells, *Int. J. Biol. Macromol.*, 72 (2015) 1391-1401. <https://doi.org/10.1016/j.ijbiomac.2014.10.039>.
- [21] A. Manosroi, J. Manosroi, Micro encapsulation of human insulin DEAE-dextran complex and the complex in liposomes by the emulsion non-solvent addition method, *J. Microencapsulation*, 14 (1997) 761-768. <https://doi.org/10.3109/02652049709006826>.
- [22] T. Gulick, Transfection using DEAE-dextran, *Curr. Protoc. Mol. Biol.*, 40 (1997) 9.2. 1-9.2. 10. <https://doi.org/10.1002/0471142727.mb0902s40>.
- [23] M. Huguet, R. Neufeld, E. Dellacherie, Calcium-alginate beads coated with polycationic polymers: comparison of chitosan and DEAE-dextran, *Process Biochem. (Oxford, U. K.)*, 31 (1996) 347-353. [https://doi.org/10.1016/0032-9592\(95\)00076-3](https://doi.org/10.1016/0032-9592(95)00076-3).
- [24] P. Menon, T.Y. Yin, M. Misran, Preparation and characterization of liposomes coated with DEAE-Dextran, *Colloids Surf., A*, 481 (2015) 345-350. <https://doi.org/10.1016/j.colsurfa.2015.05.036>.
- [25] B. Larsen, K. Olsen, Inhibitory effect of polycations on the transplantability of mouse leukaemia reversed by heparin, *Eur. J. Cancer*, 4 (1968) 157-162. [https://doi.org/10.1016/0014-2964\(68\)90013-3](https://doi.org/10.1016/0014-2964(68)90013-3).
- [26] E. Thorling, B. Larsen, H. Nielsen, Inhibitory effect of DEAE-dextran on tumour growth: 3. Effect of Charge Density and Molecular Size, *Acta Pathol. Microbiol. Scand., Sect. A*, 79 (1971) 81-90. <https://doi.org/10.1111/j.1699-0463.1971.tb03316.x>.
- [27] A. Kayitmazer, A. Koksall, E.K. Iyilik, Complex coacervation of hyaluronic acid and chitosan: effects of pH, ionic strength, charge density, chain length and the charge ratio, *Soft Matter*, 11 (2015) 8605-8612. <https://doi.org/10.1039/C5SM01829C>.
- [28] D. Le Cerf, A.S. Pepin, P.M. Niang, M. Cristea, C. Karakasyan-Dia, L. Picton, Formation of polyelectrolyte complexes with diethylaminoethyl dextran: Charge ratio and molar mass effect, *Carbohydr. Polym.*, 113 (2014) 217-224. <https://doi.org/10.1016/j.carbpol.2014.07.015>.
- [29] B. Aricha, I. Fishov, Z. Cohen, N. Sikron, S. Pesakhov, I. Khozin-Goldberg, R. Dagan, N. Porat, Differences in membrane fluidity and fatty acid composition between phenotypic variants of *Streptococcus pneumoniae*, *J. Bacteriol.*, 186 (2004) 4638-4644. <http://doi.org/10.1128/JB.186.14.4638-4644.2004>.

- [30] J. Burdřková, F. Mravec, M. Pekař, The formation of mixed micelles of sugar surfactants and phospholipids and their interactions with hyaluronan, *Colloid Polym. Sci.*, 294 (2016) 823-831. <https://doi.org/10.1007/s00396-016-3840-8>.
- [31] H. Morikawa, Y. Morishima, S. Motokucho, H. Morinaga, H. Nishida, T. Endo, Synthesis and association behavior of cationic amphiphilic copolymers consisting of quaternary ammonium and nonionic surfactant moieties, *J. Polym. Sci., Part A: Polym. Chem.*, 45 (2007) 5022-5030. <https://doi.org/10.1002/pola.22322>.
- [32] T. Akagi, P. Piyapakorn, M. Akashi, Formation of unimer nanoparticles by controlling the self-association of hydrophobically modified poly(amino acid)s, *Langmuir*, 28 (2012) 5249-5256. <https://doi.org/10.1021/la205093j>.
- [33] V. Kabanov, A. Zezin, A new class of complex water-soluble polyelectrolytes, *Makromol. Chem.*, 6 (1984) 259-276. <https://doi.org/10.1070/RC1982v051n09ABEH002921>.
- [34] Z. Souguir, S. Roudesli, E. About-Jaudet, L. Picton, D. Le Cerf, Novel cationic and amphiphilic pullulan derivatives II: pH dependant physicochemical properties, *Carbohydr. Polym.*, 80 (2010) 123-129. <https://doi.org/10.1016/j.carbpol.2009.11.003>.
- [35] E. Tsuchida, Formation of polyelectrolyte complexes and their structures, *J. Macromol. Sci., Part A: Pure Appl. Chem.*, 31 (1994) 1-15. <https://doi.org/10.1080/10601329409349713>.
- [36] M. Müller, B. Keßler, J. Fröhlich, S. Poeschla, B. Torger, Polyelectrolyte complex nanoparticles of poly (ethyleneimine) and poly (acrylic acid): preparation and applications, *Polymers*, 3 (2011) 762-778. <https://doi.org/10.3390/polym3020762>.
- [37] S.V. Raik, E.R. Gasilova, N.V. Dubashynskaya, A.V. Dobrodumov, Y.A. Skorik, Diethylaminoethyl chitosan-hyaluronic acid polyelectrolyte complexes, *Int. J. Biol. Macromol.*, 146 (2020) 1161-1168. <https://doi.org/10.1016/j.ijbiomac.2019.10.054>.
- [38] R. Zhang, B. Shklovskii, Phase diagram of solution of oppositely charged polyelectrolytes, *Phys. A (Amsterdam, Neth.)*, 352 (2005) 216-238. <https://doi.org/10.1016/j.physa.2004.12.037>.
- [39] Malvern Panalytical, Understanding the colloidal stability of protein therapeutics using dynamic light scattering, 2020. <https://cdn.technologynetworks.com/TN/Resources/PDF/Whitepaper%20BP%20SP%201.pdf>
- [40] S. Bhattacharjee, DLS and zeta potential-what they are and what they are not?, *J. Controlled Release*, 235 (2016) 337-351. <https://doi.org/10.1016/j.jconrel.2016.06.017>.
- [41] R.B. Best, G.E. Jackson, K.J. Naidoo, Molecular dynamics and NMR study of the  $\alpha$  (1 $\rightarrow$ 4) and  $\alpha$  (1 $\rightarrow$ 6) glycosidic linkages: maltose and isomaltose, *J. Phys. Chem. B*, 105 (2001) 4742-4751. <https://doi.org/10.1021/jp0040704>.
- [42] P.A. Williams, G.O. Phillips, Introduction to food hydrocolloids, in: G.O. Phillips, P.A. Williams (Eds.), *Handbook of Hydrocolloids*, Woodhead Publishing, Cambridge, 2009, pp. 1-22. <https://doi.org/10.1533/9781845695873.1>.
- [43] L. Li, A.M. Romyantsev, S. Srivastava, S. Meng, J.J. de Pablo, M.V. Tirrell, Effect of solvent quality on the phase behavior of polyelectrolyte complexes, *Macromolecules*, 54 (2020) 105-114. <https://doi.org/10.1021/acs.macromol.0c01000>.
- [44] L. Li, S. Srivastava, S. Meng, J.M. Ting, M.V. Tirrell, Effects of non-electrostatic intermolecular interactions on the phase behavior of pH-sensitive polyelectrolyte complexes, *Macromolecules*, 53 (2020) 7835-7844. <https://doi.org/10.1021/acs.macromol.0c00999>.
- [45] H. Dautzenberg, Polyelectrolyte complex formation in highly aggregating systems. 1. Effect of salt: polyelectrolyte complex formation in the presence of NaCl, *Macromolecules*, 30 (1997) 7810-7815. <https://doi.org/10.1021/ma970803f>.

[46] E. Hergli, A. Aschi, Polycation-globular protein complex: Ionic strength and chain length effects on the structure and properties, *e-Polymers*, 19 (2019) 120-128. <https://doi.org/10.1515/epoly-2019-0014>.



HA



DEAE-D



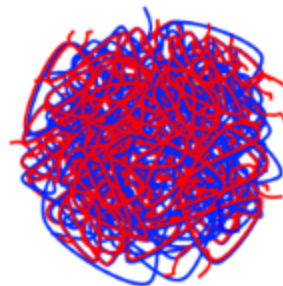
?

Effects of intrinsic factors

Effects of extrinsic factors

?

HA/DEAE-D PECs



Physicochemical  
characterization